Jyväskylän yliopiston julkaisuarkisto
Jyväskylä University Digital Archive

UNIVERSITY OF JYVÄSKYLÄ

This is an electronic reprint of the original article.
This reprint *may differ* from the original in pagination and typographic detail.

Author(s): Huttunen, Moona; Turkki, Paula; Mäki, Anita; Paavolainen, L.; Ruusuvuori, P.; Marjomäki, Varpu

Title: Echovirus 1 internalization negatively regulates epidermal growth factor receptor downregulation

Year: 2017

Version:

Please cite the original version:

Huttunen, M., Turkki, P., Mäki, A., Paavolainen, L., Ruusuvuori, P., & Marjomäki, V. (2017). Echovirus 1 internalization negatively regulates epidermal growth factor receptor downregulation. Cellular Microbiology, 19(3), Article e12671. https://doi.org/10.1111/cmi.12671

All material supplied via JYX is protected by copyright and other intellectual property rights, and duplication or sale of all or part of any of the repository collections is not permitted, except that material may be duplicated by you for your research use or educational purposes in electronic or print form. You must obtain permission for any other use. Electronic or print copies may not be offered, whether for sale or otherwise to anyone who is not an authorised user.

Echovirus 1 internalization negatively regulates EGFR down-regulation

Moona Huttunen[1], Paula Turkki[1], Anita Mäki[1], Lassi Paavolainen[2], Pekka Ruusuvuori[3], and Varpu Marjomäki[1*]

[1]Department of Biological and Environmental Science/NanoScience Center, University of Jyväskylä, Survontie 9, 40500 Jyväskylä, Finland

[2]Institute for Molecular Medicine Finland, University of Helsinki, Helsinki, Finland

[3]Tampere University of Technology, Pori & Institute of Biosciences and Medical Technology, University of Tampere, Finland

Running Title: EV1 induced EGFR Down-Regulation

Keywords: Enterovirus, epidermal growth factor receptor (EGFR), endocytosis, degradation, signaling

*Corresponding author: PhD Varpu Marjomäki

Address: Department of Biological and Environmental Science/NanoScience Center, Survontie 9, 40500 Jyväskylä

Telephone: +358 40 563 44 22

E-mail: varpu.s.marjomaki@jyu.fi

This article has been accepted for publication and undergone full peer review but has not been through the copyediting, typesetting, pagination and proofreading process which may lead to differences between this version and the Version of Record. Please cite this article as doi: 10.1111/cmi.12671

This article is protected by copyright. All rights reserved.

Abstract

We have demonstrated previously that the human picornavirus Echovirus 1 (EV1) triggers an infectious internalization pathway that follows closely, but seems to stay separate from the EGFR pathway triggered by EGF. Here we confirmed by using live and confocal microscopy that EGFR and EV1 vesicles are following intimately each other but are distinct entities with different degradation kinetics. We show here that despite being sorted to different pathways and located in distinct endosomes, EV1 inhibits EGFR down-regulation. Simultaneous treatment with EV1 and EGF led to an accumulation of EGFR in cytoplasmic endosomes, which was evident already 15 min p.i. and more pronounced after 2 h p.i.. EV1 treatment led to reduced down-regulation, which was proven by increased total cellular amount of EGFR. Confocal microscopy studies revealed that EGFR accumulated in large endosomes, presumably macropinosomes, which were not positive for markers of the early, recycling or late endosomes/lysosomes. Interestingly, EV1 did not have a similar blocking effect on bulk endosomal trafficking or transferrin recycling along the clathrin pathway suggesting that EV1 did not have a general effect on cellular trafficking pathways. Importantly, EGF treatment increased EV1 infection and increased cell viability during infection. Simultaneous EV1 and EGF treatment seemed to moderately enhance phosphorylation of PKCα. Furthermore, similar phenotype of EGFR trafficking could be produced by PMA treatment further suggesting that activated PKCα could be contributing to EGFR phenotype. These results altogether demonstrate that EV1 specifically affects EGFR trafficking, leading to EGFR down-regulation, which is beneficial to EV1 infection.

This article is protected by copyright. All rights reserved.

Introduction

We have shown previously that the members of enterovirus group B viruses such as Echovirus 1 (EV1) and coxsackievirus A9 (CVA9) trigger their own entry pathway to cells (Karjalainen *et al.* 2008;Karjalainen *et al.* 2011;Marjomaki *et al.* 2002;Pietiainen *et al.* 2004;Rintanen *et al.* 2012;Upla *et al.* 2004;Heikkila *et al.* 2010;Huttunen *et al.* 2014). This involves clathrin-independent and macropinocytosis-like entry to endosomes, which quickly develop into neutral multivesicular bodies (MVBs). Similarly, the epidermal growth factor receptor (EGFR) uses partially similar kind of macropinocytic entry and delivery to MVBs. The greatest difference of the nature of their MVBs is the fact that enterovirus-endosomes do not acidify (Karjalainen *et al.* 2011;Rintanen *et al.* 2012;Huttunen *et al.* 2014) and avoid targeting to the lysosomes whereas EGFR is efficiently taken to acidic lysosomes for degradation (Wiley *et al.* 1991). Thus these two endosomal populations have different fates in the cell despite the morphological similarity of the endosomes.

EV1 like many other enteroviruses uses common cell surface protein, such as an integrin (α2β1 integrin) as its cellular receptor. Specific plasma membrane (PM) domains, lipid rafts, have been shown to gather both adhesion receptors and growth factor receptors to the same PM regions leading to close association between e.g. α2β1 integrin and the EGFR (Ivaska and Heino 2011). EV1 receptor α2β1 integrin resides very close to EGFR on the PM and have been shown to collaborate at different levels and even co-immunoprecipitate with each other (Yu *et al.* 2000;Moro *et al.* 2002;Mattila *et al.* 2005).

EGFR plays an important role in essential cellular functions such as cellular proliferation and migration. Conformational change, caused by ligand (EGF) binding, activates the receptor and leads to receptor dimerization and internalization (Ogiso *et al.* 2002). The activation of EGFR leads to accelerated internalization and degradation of the receptor in lysosomes (Wiley *et al.* 1991). This receptor down-regulation is the major negative feedback regulatory mechanism that controls the intensity and duration of receptor signaling (Wells *et al.* 1990), although EGF-receptor complexes are suggested to remain active and to signal also in endosomes (Wiley 2003;Platta and Stenmark 2011). EGFR activation has been shown to lead to efficient internalization through both clathrin and clathrin-independent pathways (Wiley. 1988; Sorkin and Goh 2008;Lund *et al.* 1990). It has also been suggested that stimulation with a high EGF concentration leads to macropinocytic internalization of EGFR (Hewlett *et al.* 1994;Hamasaki *et al.* 2004;Liberali *et al.* 2008). Despite of the internalization pathway, equilibrium between receptor recycling and degradation balances the EGFR availability and signaling.

This article is protected by copyright. All rights reserved.

We have previously shown that the triggered enterovirus- endocytosis pathway leads to down-regulation of its receptor integrin with clearly slower kinetics than the degradation of EGFR (Marjomaki *et al.* 2002;Pietiainen *et al.* 2004;Upla *et al.* 2004;Karjalainen *et al.* 2008;Karjalainen *et al.* 2011;Rintanen *et al.* 2012). EGFR shows much faster down-regulation in acidic Lamp1-positive lysosomes in contrast to much slower degradation of α2β1 integrin in more neutral MVBs that do not contain canonical endosomal markers (Rintanen *et al.* 2012).

Here we show that despite the fact that EV1 and EGF trigger entry to distinct endosomes, EV1 has a clear negative regulatory effect on EGFR down-regulation. We show that EV1 causes an accumulation of endosomal EGFR and delayed down-regulation of EGFR.

Results

EV1 treatment leads to accumulation of EGFR in the cytoplasm.

On the cell surface, EGFR has been shown to reside close to the EV1 receptor, α2β1 integrin, and to even co-immunoprecipitate together (Yu *et al.* 2000;Moro *et al.* 2002;Mattila *et al.* 2005). Here, we followed the internalization of EGFR elicited during EV1 infection and EGF stimulation. After starving the cells for 2 h in serum-free medium, the cells were treated with cycloheximide (to inhibit the protein synthesis), EGF (100 ng/ml) and EV1. After 15 min and 2 h incubations, the infected cells were labeled with antibodies against EGFR and EV1. Confocal fluorescence microscopy showed that after 15 min, both EV1 and EGFR were located in the cell periphery in high number of vesicles (Fig. 1A). After 2 h the EGFR structures were less numerous but closer to the cell center, as expected. After 2 h internalization, EGFR is suggested to undergo degradation leading to a reduction of the EGFR signal.

The location of EV1 was often very close to the EGFR vesicles after 15 min but after 2 h EV1 was still more scattered and more clearly separated from EGFR vesicles (Fig. 1A). Colocalization analysis between EV1 and EGFR showed that approximately 30% of the signals had overlap with each other. The overlap of the vesicles seemed very marginal in the images suggesting that the colocalization may be biased by the close proximity of the vesicles and limited resolution. After 2 h time point, the quantified colocalization was clearly reduced, about 18%, probably because the stronger movement of EGFR to the perinuclear region in comparison to EV1 separated the vesicles more efficiently leading to smaller amount of false colocalization (Fig. 1B). The labeling of EGFR in cells without EV1 treatment showed

This article is protected by copyright. All rights reserved.

similar localization of vesicles after 15 min and 2 h (Fig. 1C). However, the images suggested that during EV1 treatment EGFR showed higher intensity after 2 h than without EV1. Quantification of the EGFR signal after 15 min and 2 h with or without EV1 showed clear differences in the fate of EGFR: without EV1 EGFR signal dropped to about half of the original signal whereas during EV1 treatment the EGFR signal accumulated in vesicles leading to doubling of the intensity in vesicles (Fig.1 D).

In order to further confirm the effect on EGFR, we triggered the virus pathway by clustering the receptor by antibodies in another cells line, SAOS-$\alpha 2\beta 1$ cells. We have shown before that the receptor clustering with antibodies faithfully mimicks virus –induced integrin clustering and internalization to the cells (Upla *et al.* 2004;Karjalainen *et al.* 2008). In addition to the typically used high amount of EGF (100 ng/ml) we also wanted to verify if this effect on EGFR was occurring with a lower amount (1 ng/ml). We followed the EGFR signal after virus receptor clustering for 15 min and 2 h (Fig. 1 E). With both doses of EGF, the EGFR signal stayed approximately 2.5-fold higher after 2 h with receptor clustering whereas EGFR signal reduced in both cases without clustering (Fig 1E). The results thus showed that EGFR accumulation was observed with antibody-induced receptor clustering and with both low and high EGF amounts although different signal intensities were gained due to the different cell type used. However, the intensity of EGFR signal in the vesicles internalized for 15 min was higher with the higher EGF dose. Interestingly, receptor clustering via both EV1 treatment and antibodies also reduced the internalized amount after 15 min suggesting that in addition to EGFR signal accumulation in the cytoplasm, these treatments reduced the uptake of EGFR during EGF signaling (Figs. 1 D, E).

Earlier, we had observed moderate increases of viral infection by adding EGF and comparing to full serum control (Karjalainen *et al.* 2011). Here, after overnight starvation, low (0.1 nM) and high (100 nM) EGF increased EV1 infection with about the same efficiency as compared to 10% serum conditions (Fig. 1F, ctrl+serum). When compared to the starved cells without growth factor stimulation the infectivity in all cases increased by about 2 –fold suggesting that both low and high amounts of EGF increased the number of infected cells. The same effect was gained by 10% serum conditions containing high amounts of various growth factors. Furthermore, we evaluated the effect of both low and high amounts of EGF on the ATP levels of infected cells (Fig. 1G). The ATP levels very sensitively describe the viability status of cells, and if increased, it means that cell death is postponed during virus infection. Indeed, the ATP levels were moderately increased after 20 h p.i. in

This article is protected by copyright. All rights reserved.

infected cells suggesting that EGF improved cell viability giving the infection more time to produce progeny virus. These results altogether indicate that EGF stimulation contributes to the success of EV1 viral infection.

EV1 and EGFR pathways are separate after internalization

We next set out to perform live imaging of the vesicle populations in order to more dynamically observe the two vesicle populations and study their association in more detail. As it was easier to follow the virus pathway dynamically by labeling its receptor, we set out to cluster the virus receptor α2 integrin with the clustering fluorescent secondary antibody as described before ((Karjalainen *et al.* 2008); see also the Material and Methods section). We followed the clustered α2 integrin and biotinylated EGF in wide-field microscopy during the internalization observation period from 20 to 35 min p.i (Fig 2A-C, Movie 1). The video showed that two vesicle populations associated often close to each other and moved around each other a long time. The vesicles kept close to each other, often within a 200 nm distance, but were quite clearly separate entities as some vesicles moved transiently further apart and came back closer together. Colocalization of the live data was measured every 5.8 second, and the results showed a very similar average result, 29% as with the confocal data (Fig. 2B). Measurement of the association of these vesicles showed much higher values leading to values of 60 to 70%. The association algorithm detects vesicles that are in the close vicinity to each other but not necessarily colocalizing well with each other, which seems to be the case here. Furthermore, detailed imaging of one vesicle pair during a one minute time period demonstrated that movement of the vesicles around each other was leading to false colocalization signal at locations where vesicles were temporarily on top of each other (Fig 2C; and Movie 2). Detailed colocalization values during a 1 min imaging starting from 20 min p.i. revealed that in the 5^{th} and the 6^{th} frame and again in the 9^{th} frame the colocalization was zero but at other frames varied between the minimum 0% and the maximum of 29% (Fig. 2C). As a control we performed live imaging of α2β1 integrin labeled with two Alexa dyes, a situation which should lead to higher colocalization as vesicles should accumulate integrin with both colors. These vesicles were followed during a 30 min internalization time with 30 second intervals. Quantification of this data showed around 60 to 70% colocalization values for the data. The association values showed rather similar results (around 80%) suggesting that the association in this case measured quite faithfully colocalization of the signals.

This article is protected by copyright. All rights reserved.

Collectively, these results confirm that the vesicles trafficking EV1 and its receptor are closely associated but do not significantly colocalize with EGFR-positive vesicles during internalization. In addition, EV1 receptor clustering during infection and antibody treatment leads to lower initial uptake of EGFR but accumulation of EGFR in later time points.

EV1 treatment slows down EGFR down-regulation.

As the EGFR signal seemed to stay higher during virus and receptor internalization we set out to study the EGFR signal in more detail. We first monitored the effect of EV1 on EGFR internalization without additional EGF stimulation. We infected serum-starved (and cycloheximide treated) A549 cells with EV1 and monitored EGFR internalization with double labeling of the surface and intracellular receptor pools. Briefly, after 15 min virus incubation, the samples were gently fixed on ice with PFA and labeled first for the surface EGFR pool and subsequently for the intracellular EGFR pool: before TX-100 permeabilization, surface EGFR was labeled with anti-EGFR antibody and fluorescent secondary antibody (Alexa Fluor (AF)-488). Next, cells were permeabilized and both surface and internalized EGFR molecules were labeled with anti-EGFR antibody and secondary fluorescent antibody (AF-555). As the results show, EV1 treatment for 15 min led to a notably higher surface signal and lower intracellular signal of EGFR (Fig 3A). Thus, without EGF stimulation EV1 seems to lower internalization and cause accumulation of EGFR on the cell surface.

We next set out to monitor the effects of EV1 treatment on EGFR under EGF-stimulation. First we observed A549 cells without EV1 during EGF stimulation (Fig 3B, upper row). Stimulation of EGFR with EGF caused an appearance of large EGFR positive vesicles within 15 min in the cytoplasm. EGFR signal decreased significantly after 2 h and kept low after 4 h in non-EV1 treated samples. In contrast, simultaneous treatment with EGF and EV1 suggested a higher surface EGFR pool at 15min p.i. and the intracellular pool remained abundant after 2 h and 4 h when compared to EGF treated cells alone (Fig 3B).

Quantification of the surface and internalized signals showed that compared to starved cells, EV1 treatment enhanced the surface EGFR pool by four-fold at 15min p.i.. (Fig 3C). However, due to the high variation in the case of EV1, the result was not statistically different from the control situation. The quantified intracellular pool after EV1 treatment was significantly higher ($p=0.006$) than after EGF alone at 2 h p.i. (Fig 3D). In addition, during EGF stimulation, EV1 caused a higher pool of EGFR to accumulate in the cytoplasm after 2 h compared to EGF stimulation only ($p=0.011$) (Fig 3D). As there was no increase of the

This article is protected by copyright. All rights reserved.

surface EGFR pool due to EV1 after 2 and 4 h treatments (Fig 3C) it indicates that the increase of the intracellular EGFR pool during EV1 treatment was most probably due to slowing down of the intracellular EGFR degradation.

In conclusion, although EV1 and EGFR were not internalized into the same endocytic structures, EV1 nevertheless had an effect on the turnover of EGFR by decelerating the degradation of EGFR.

EV1 treatment has no effect on transferrin recycling or overall fluid phase uptake.

As EV1 may have affected the cellular trafficking in a more general manner, we wanted to study if EV1 had an effect on major endocytosis and recycling pathways. First we set out to study if the transferrin (TF) recycling pathway was affected. A549 cells were first treated with or without EV1 at 0 min, 30 min and 2 h time points, and then the fluorescently labeled TF (TF-488) was added on cells, and incubated for 30 min. After fixation and cell permeabilization, the early endosomes were labeled with EEA1-antibody and AF-555 secondary antibody to check if TF recycling was blocked at the level of early endosomes. The confocal images and detailed colocalization measurements from those showed that there was no apparent increase in the colocalization along time between TF and EEA1 in cells with or without EV1 (Fig. 4A). If there would have been a defect in recycling this could have led to an increase in colocalization of TF with EEA1. Alternatively, transferrin could accumulate in recycling endosomes leading to enlarged structures. However, since the size of TF-positive vesicles stayed the same and TF was not accumulated into EEA-positive endosomes, the results suggest that transferrin recycling was not affected.

We then continued checking if the entry to the lysosomal pathway was affected by EV1, by following the fluid phase entry of mouse IgG. The early part of the fluid-phase uptake pathway from the cell surface to the sorting early endosomes is shared by receptors on the clathrin pathway, e.g. transferrin receptor. If there would be changes in the early uptake, it would be seen also in the levels of IgG uptake. After internalization, IgG molecules are either recycled back to PM or down-regulated in lysosomes (Ward *et al.* 2003). We were interested if EV1 infection had any effect in the overall trafficking and fate of IgG. High dose of IgG (1 mg/ml) was added on cells (treated with or without EV1) for a 15 min pulse at 2 and 4 h p.i., and then chased for 20 min. The quantifications from the confocal images showed no statistically significant change in the fate of the fluid phase marker pulse and chase at 2 and 4 h time points during EV1 infection compared to the control situation (Fig 4B). These results thus suggest that EV1 internalization has no major effect in the overall fluid-phase trafficking

This article is protected by copyright. All rights reserved.

in A549 cells. EV1 does not lower the amount of fluid-phase taken up by the clathrin pathway, and it does not cause any apparent accumulation of the internalized IgG or transferrin.

Alterations in EGFR colocalization with endosomal markers after EV1 treatment.

Since our results suggested that EV1 infection decelerated the degradation of EGFR, we were interested to see whether this was reflected in EGFR colocalization with early endosomal (EEA1), recycling endosomal (Rab11), late endosomal (Rab7) or late endosomal/lysosomal (Lamp1) markers. The extent of colocalization was studied from confocal images using the colocalization algorithm embedded in the BioImageXD software. Detailed measurements showed that EGFR colocalized to some extent with EEA1-positive endosomes after 15 min (Fig. 5A). The colocalization was much lower after 1 and 2 h as expected (Fig. 5A). EV1 internalization did not change this colocalization ratio suggesting that the early endosomal trafficking was not affected by the virus treatment. Similarly, the colocalization between Rab11 and EGFR kept rather low in all conditions suggesting that the recycling pathway was not remarkably used during these treatments (Fig 5B). The same was true with colocalization of EGFR with Rab7, which was not changed due to EV1 infection (Fig. 5C). However, the results with lysosomal marker Lamp1 showed lower colocalization with EGFR in response to virus treatment at 1 h p.i ($p = 0.046$) suggesting lower access to the degradative structures (Fig 5D). The 4 h time point suggested a similar phenomenon but did not quite reach statistical significance ($p = 0.09$).

Altogether these results suggest that EGFR trafficking follows the same endosomal pathway with or without EV1 treatment. EGFR is targeted to Lamp1 positive lysosomes largely via macropinocytosis as has been shown before (Liberali *et al.* 2008), and therefore may bypass the classical early and late endosomes prior to lysosomes. However, we noticed a small reduction in the amount of EGFR associated with the lysosomal marker suggesting a reduced delivery to the lysosomes for degradation.

EV1 showed minor effects on EGFR signaling.

As it was obvious that EV1 was not physically associated with EGFR during internalization, we set out to explore common signaling pathways associated both with EV1 and EGFR trafficking. Protein kinase C (PKC) is one of the key signaling enzymes mediating EGFR activation and, as we have shown previously, PKCα is also mildly activated by EV1 induced integrin clustering in the presence of low amount of serum (Upla *et al.* 2004). By SDS-PAGE

This article is protected by copyright. All rights reserved.

and western blotting, we found that EGF induced the cellular phosphorylation status of PKCα as expected (Fig. 6A). Without EGF stimulation (or serum addition), EV1 could not much induce PKCa phosphorylation. However, after the treatment of A549 cells with both EGF and EV1 present, the pPKCα activity showed higher mean values for phosphorylation in all time points. However, perhaps partially due to the presence of small amount of uninfected cells in the data contributing to high variance in the results, there was no statistical difference between EGF and combined EGF/EV1 treatments. We also performed immunofluorescent labeling of phosphorylated PKCα and EGFR to visualize by microscopy the phosphorylation status of PKCα (Supplemental Figure 1). The images with treatment of cells with both EGF and EV1 suggested higher cytoplasmic activity than in other treatments further suggesting additive effects of EGF and EV1.

Phosphorylated EGFR molecules activate multiple signal transduction pathways, including the mitogen-activated protein kinase (MAPK) signaling cascade, and the phosphoinositide 3-kinase (PI3K) pathway, which recruits Akt/PKB to the plasma membrane (Lill and Sever. 2012). The phosphorylation status of two different signaling proteins, Akt and p44/42 (phosphorylated MAPK) were followed to evaluate the activity of EGFR signaling in cells. After EGF stimulation, Akt showed higher phosphorylation status in comparison to starved cells after 15 min and 2 h but the induction after 4 h was not statistically significant anymore (Fig. 6A). EV1 treatment alone could not activate Akt or p44/42 as the phosphorylation status kept lower than the EGF stimulated control samples in all time points. However, after the simultaneous treatment with EGF and EV1, the cells showed higher mean values for pAkt activity after 2 and 4 h in comparison to EGF treatment alone. This result, which was however not statistically significant, could suggest prolonged signaling in the virus treated cells due to prolonged EGFR residence in endosomes. The p44/42 MAPK phosphorylation status showed rather similar results. The mean values for phosphorylation of MAPK kept lower after EV1 treatment and higher after EGF treatment. The simultaneous treatment of EV1 and EGF increased the mean value of kinase phosphorylation status after 2 h (Fig. 6A). These tentative results suggest that the virus-induced deceleration of EGFR down-regulation may lead to prolonged activation of EGFR signaling.

As a control we also tested the direct effect of PKC activation on EGFR vesicles using phorbol 12-myristate 13-acetate (PMA) as a pan PKC activator. PMA was not able to induce internalization and accumulation of EGFR without EGF stimulation in starved cells (data not shown). However, in the presence of EGF stimulation PKC activation increased

This article is protected by copyright. All rights reserved.

uptake of EGFR and also retained approximately the same EGFR signal in the cytoplasmic vesicles even after 2 h whereas without PMA the EGF signal typically was greatly reduced (Fig. 6D). These results thus suggest that the increased PKC activation is contributing to the accumulation of EGFR in the cytoplasm and is analogous to what we see during a combined treatment of EV1 and EGF stimulation.

Discussion

We showed in this study that the human pathogen, Echovirus 1 (EV1) has a specific effect on epidermal growth factor receptor (EGFR) internalization pathway while its effects are negligible on transferrin recycling or fluid phase uptake via the clathrin pathway. How could EV1 effect EGFR pathway with such specificity, and how could it exert its effect as the virus and EGFR stay in separate endosomal populations after internalization?

EV1 uses α2β1 integrin as its cellular receptor (Bergelson *et al.* 1992). EV1 clusters the integrin upon binding to several I domains of nearby integrins on the cell surface, which in turn causes an efficient internalization of the virus-receptor complex to peripheral endosomes (Marjomaki *et al.* 2002;Pietiainen *et al.* 2004;Upla *et al.* 2004;Karjalainen *et al.* 2008;Karjalainen *et al.* 2011;Rintanen *et al.* 2012). On the cell surface, EGFR has been shown to co-immunoprecipitate integrins such as α2β1 integrin, demonstrating how closely they are connected on the plasma membrane (Yu *et al.* 2000;Moro *et al.* 2002;Mattila *et al.* 2005). Integrins in general have been shown to orchestrate growth factor receptor endocytosis and trafficking and leading to effects on their signaling (Caswell *et al.* 2008;Caswell *et al.* 2009). Previously, integrins were suggested to function as negative regulators for EGFR signaling (Mattila *et al.* 2005). From our data it was clear that without EGF stimulation, EV1 treatment stalled EGFR internalization and caused accumulation of the receptor on the cell surface. Virus infection did not inhibit EGFR entry to cytoplasmic vesicles during EGF stimulation, under both low and high amounts of EGF stimulus. However, virus infection caused a clear accumulation of EGFR positive endosomes in the cytoplasm under both high and low amount of EGF stimulation.

EV1 and EGF stimulation lead to two separate populations of endosomes in the cytoplasm although these populations stayed very close to each other. Quantification of colocalization as well as live imaging demonstrated that there is no physical association between these two populations. In line with these results, we have shown in previous studies using quantitative confocal microscopy that EV1 internalization pathway stays outside the

This article is protected by copyright. All rights reserved.

acidic lysosomal clathrin pathway whereas EGFR is targeted to lysosomal degradation (Rintanen *et al.* 2012;Wiley *et al.* 1991). When we measured the intraendosomal pH of virus and integrin containing vesicles we observed pH close to neutral values whereas EGFR containing endosomes showed much lower pH values already after 1 and 2 h post internalization further demonstrating that EV1 and EGFR reside in distinct endosomes (Rintanen *et al.* 2012;Karjalainen *et al.* 2011). However, in case a different pH and degradation kinetics could be maintained at different domains of an organelle, it still remains a possibility that EV1 and EGFR could travel in a larger organelle if the various domains could be kept quite distinct from each other. We were not able to see any apparent accumulation of EGFR in conventional early and late endosomes suggesting that trafficking to lysosomes in our study occurred mostly via macropinosomes as has been suggested before (Liberali *et al.* 2008). However, we did notice a small decrease of EGFR targeting to the lysosomal compartment further suggesting that EGFR was halted in endosomes before the degradative lysosomes.

The observed block in EGFR degradation could be best explained by the tentative activation and effects through PKCα. It was shown previously that PKC activation using the pan activator phorbol myristate acetate (PMA) causes a degradation defect in EGFR through increased phosphorylation of Thr654 in EGFR (Bao *et al.* 2000). We have shown already in our earlier studies that α2β1 integrin clustering induced by EV1 infection or antibody treatment increases mildly the PKCα activation (Turkki *et al.* 2013;Upla *et al.* 2004). Importantly, in this study, we could reproduce the EGFR accumulation in endosomes and reduced degradation using the PMA treatment suggesting that the observed effects could be due to PKC activation. As we also observed retarded targeting of EGFR to Lamp1 positive lysosomes, it thus seems probable that EV1 infection causes a block in the lysosomal targeting due to PKC activation in the close vicinity of EGFR.

Why would EV1 have evolved to induce prolonged EGF localization and tentatively prolonged signaling in cells during viral infection? Enteroviruses have a rather short life cycle producing viral particles and cell lysis during 6 to 10 hours p.i. In order to optimize the virus production with a proper timing for cell lysis it may be beneficial to manipulate both the pro-survival and pro-apoptotic pathways in a right order (Cooray 2004). This may explain the fact that both kind of pathways have been linked to enterovirus infection with various effect during early or late infection. Akt activation has been found beneficial for both Coxsackievirus B3 (CVB3) and enterovirus 71 (EV1) while inhibition of Akt signaling was shown to lead to premature apoptosis and lysis of cells (Esfandiarei *et al.* 2004;Wong *et al.*

This article is protected by copyright. All rights reserved.

2005;Zhang *et al.* 2014). Indeed, for EV1, EGF stimulation increased both the number of infected cells and kept higher ATP levels in cells suggesting that prolonged EGF localization in endosomes is beneficial for EV1.

Altogether our results here show that EV1 internalization leads to reduced down regulation of the receptor due to inhibited targeting to the lysosomes. These phenomena may be acted via PKCα since PKC activation has been reported to divert EGFR from the degradation pathway to the recycling pathway (Bao *et al.* 2000), and this phenotype was reproduced by PMA or combined EV1 /EGF treatments in this study. Furthermore, based on higher cell viability and increased number of infected cells, EV1 was shown to benefit from EGF stimulation.

Materials and methods

Cells, Viruses and Antibodies. The human lung carcinoma A549 cell line was obtained from the American Type Culture Collection (ATCC, Wesel, Germany). The cells were maintained in Dulbecco's modified Eagle's medium (DMEM, Life Technologies, Paisley, UK) containing 5% fetal bovine serum (FBS, Life Technologies), supplemented with penicillin and streptomycin (Life Technologies). Experiments were also performed using a human osteosarcoma cell line, overexpressing the α2 integrin subunit (SAOS-α2β1 cells, clone 45) as described previously (Siljamaki *et al.* 2013). The levels of α2β1 in both these cell lines are rather comparable (See Supplementary Figure 1 in Siljamäki et al. 2013).

EV1 (Farouk strain; ATCC) was produced and purified as described previously (Marjomaki *et al.* 2002). Culture medium for virus infections was supplemented with 1% FBS. For all infection studies, MOI 100 was used. Typically it leads to 50-70% infection in the A549 cells at 6 h pi without cycloheximide treatment. Serum starvations were done in DMEM without adding any FBS or antibiotics (0% DMEM). EGF stimulations were done with 100 ng/ml EGF (Molecular Probes, product number E-3476, Life Technologies) in the presence of cycloheximide (10 µg/ml, Sigma-Aldricht C7698, Helsinki, Finland).

The following antibodies were used: rabbit antisera against purified EV1 (Marjomaki *et al.* 2002) , monoclonal antibody against α2 integrin (A211EV10 from Dr. Fedor Berditchevski, Institute of Cancer studies, Birmingham, UK), anti-EGFR antibody (produced in rabbit, Santa Cruz Biotechnologies, product number sc-03, Heidelberg, Germany), anti-EGFR antibody (produced in mouse, Thermal Scientific, product number MS-396, Amarillo, Texas, USA),

This article is protected by copyright. All rights reserved.

Alexa Fluor (AF) 488- and 555-labeled anti-mouse and anti-rabbit secondary antibodies produced in goat, and the ProLong® Gold antifade reagent were from Invitrogen (Life Technologies). Transferrin-488 (Life Technologies T-13342), early endosome antigen 1 (EEA1, MAb; BD Transduction Laboratories, catalog item 610457, Vantaa, Finland), Lamp1, to identify late endosomes and lysosomes (MAb, Santa Cruz Biotechnology, product item sc-20011), Rab7, to identify a member of the Rab family of small guanosine triphosphatases (GTPases) Rab7 (Polyclonal antibody produced in rabbit, Sigma-Aldrich, product item R4779), anti-pAkt (Cell Signaling, #4060P, Danvers, MA, USA), anti-P-p44/42 (Cell signaling #4370P), anti-Akt1 (produced in mouse, sc-5298), anti-pPKCα (produced in rabbit, Millipore 07-790), anti-PKCa (produced in mouse, Transduction laboratories #610107), anti-MAPK (produced in rabbit, New England Biolabs,#9102), rabbit anti-mouse IgG (Sigma-Aldricht A9044).

Cell viability tests

Cell viability was measured from infected cells in 96 well plates using a Cell Titre Glo assay (CTG; Promega, Southampton, UK) according to manufacturers instructions. Luminescence was read with Victor X4 2030 multiplate reader (Perkin Elmer).

Immunofluorescence and Confocal Microscopy. A549 cells were grown on coverslips to subconfluency. The cells were serum starved for 2 h in 0% DMEM after which they were incubated with or without EGF (100 ng/ml) and/or EV1. After incubation at 37°C, the cells were fixed with 4% paraformaldehyde (PFA) for 20 min, permeabilized with 0.2% Triton X-100 (TX-100) for 5 min, and stained with antibodies (dilutions made in 3% bovine serum albumin (BSA)-PBS). In the surface labeling assay, EGFR was labeled with primary and secondary antibodies prior to the permeabilization. The cells were mounted in ProLong® Gold antifade reagent with DAPI and examined with an Olympus microscope IX81 with a FluoView-1000 confocal setup. Levels for the laser power, detector amplification, and optical sections were optimized for each channel before starting the imaging.

Live imaging. A549 cells were grown on coverglass-bottom 8-well imaging plates chambers (Nunc, Lab-Tek) and starved for 16 h in 0% DMEM. EGF stimulation and α2 integrin clustering were started with biotinylated EGF (0.5 µg/mml, Invitrogen) and integrin binding primary antibody. After 45 min ice binding, the excess biotinylated-EGF and integrin antibody were washed away and streptavidin-Alexa488 and AF 594 (Invitrogen) was added

This article is protected by copyright. All rights reserved.

(45 min on ice and washes). Cells were imaged with Zeiss Cell Observer HS wide-field microscope (in 0% DMEM, +37˚C, 5% CO_2).

Image analysis and statistical testing. An open source software package, BioImageXD (Kankaanpää *et al.* 2012), was used for the confocal and widefield image colocalization and intensity quantifications. MATLAB method described in (Ruusuvuori *et al.* 2014) was used for the association analyses.

To quantify the level of colocalization, at least 30 cells from three independent experiments, 10 cells from each, were randomly selected and optically sectioned by using a confocal microscope. Colocalization was visualized from the projection of the cell by examination of the merged images, and quantified with the BioImageXD software. The images were preprocessed with a difference of Gaussians filter to remove noise and enhance regions of interest before the colocalization analysis. Thresholds for the analysis were adjusted manually to eliminate fluorescence originating from the background and from diffuse staining. Signal overlap was expressed separately for both of the channels, as a proportion of the intensity colocalizing with the other channel. Statistical significance of observed colocalization was calculated by using Costes algorithm, embedded within the software, and only colocalizations with zero coincidence probabilities were taken into account (i.e., P = 1.00).

For measuring the intensities of the vesicles, a multistep segmentation protocol implemented within BioImageXD software was used. Images were first smoothed with the Gaussian filter and binarized by using an adaptively calculated threshold value (mean + 5) from 10 lateral pixel size radius regions. Objects were defined using the Euclidean distance transform and watershed transform. Finally, all objects of sizes smaller than 5 voxels were removed from the analysis to remove noise and small debris.

Live imaging experiment data was preprocessed with difference of Gaussians filter and thresholded with Otsu thresholding to provide masks for both of the channels. Colocalization was directly measured using the signal inside the masks. For association measurements, individual objects were first labeled using connected component labeling. The centroid of each object was then extracted for association analysis. The association was measured with point pattern matching association method (Ruusuvuori *et al.* 2014) that finds optimal matching between two point sets, in this case the two sets of object centroids extracted from the images. The maximum distance between two points considered associating was set to

This article is protected by copyright. All rights reserved.

1200 nm. The association ratio was calculated as the ratio of the number of associating objects to the number of all objects in the channel.

A t-test was used for pairwise statistical comparison between samples. For percentages or ratio figures, t-test was applied after arcsin $\sqrt{}$ transformation of the original variable to convert the binomial distribution of the data to follow normal distribution.

SDS-Polyacrylamide Gel Electrophoresis (PAGE) and Immunoblotting. Samples were prepared like described above (Immunofluorescence and confocal microscopy). After the incubations cells were scraped into Laemmli buffer and proteins were separated using 7.5% SDS-PAGE and electroblotted onto polyvinylidene difluoride membrane (Millipore, Merck Life Science). Horseradish peroxidase conjugated goat anti-rabbit and horse anti-mouse secondary antibodies (Cell signaling technologies) were used. Bands were detected by chemiluminescence (Pierce Chemical, Dallas, Texas, USA).

TF-EEA1 assay. A549 cells were grown on coverslips to subconfluency. Cells were infected with EV1 (Ctrl cells were mock infected) for 2 or 4 h. At those time points all cells were treated with TF-AF488 (0.25 mg/ml) and incubated for 30 min at 37 °C. Cells were fixed with 4% PFA, permeabilized with 0.2% TX-100 and labeled with EGFR and EEA1 antibodies plus AF-555 (labeling EEA1). The cells were mounted in ProLong® Gold antifade reagent with DAPI and examined with an Olympus microscope IX81 (Olympus, Waltham. MA, USA) with a FluoView-1000 confocal setup.

EGFR-TF colocalization assay. A549 cells were grown on coverslips to subconfluency. The cells were serum starved for 2 h in 0% DMEM after which the surface pool of EGFRs was labeled with mouse anti-EGFR antibody. The samples were treated with cycloheximide, TF-488 (0.25 mg/ml), and EV1 (mock infected cells without EV1). After 15 min and 2 h incubations at 37°C, cells were fixed with 4% PFA permeabilized with TX-100, and mounted in ProLong® Gold antifade reagent with DAPI and examined with an Olympus microscope IX81 with a FluoView-1000 confocal setup.

IgG-assay. A549 cells were grown on coverslips to subconfluency. Cells were infected with EV1 (Ctrl cells were mock infected) for 2 or 4 h. At those time points all cells were treated with IgG (mouse gamma globulin, Sigma-Aldrich, 1 mg/ml) in 0.2 % BSA/0% DMEM for

This article is protected by copyright. All rights reserved.

10 min at 37°C. After washes, cells were incubated for another 20 min at 37°C. Fixed cells (4% PFA) were permeabilized with 0.2% TX-100 and labeled with anti IgG antibody (rabbit anti-mouse IgG, Sigma-Aldricht, A9044) and secondary AF-555 antibody (Life Technologies). The cells were mounted in ProLong® Gold antifade reagent with DAPI and examined with an Olympus microscope IX81 with a FluoView-1000 confocal setup.

ACKNOWLEDGEMENTS

Funding: Academy of Finland (project 257125) and Ellen and Artturi Nyyssonen Foundation. We thank for prof. Jean Gruenberg for important discussions during the project. The authors have no conflict of interest concerning this manuscript.

REFERENCES

Bao, J., Alroy, I., Waterman, H., Schejter, E.D., Brodie, C., Gruenberg, J., *et al* (2000) Threonine phosphorylation diverts internalized epidermal growth factor receptors from a degradative pathway to the recycling endosome. J Biol Chem 275: 26178-26186.

Bergelson, J.M., Shepley, M.P., Chan, B.M., Hemler, M.E., and Finberg, R.W. (1992) Identification of the integrin VLA-2 as a receptor for echovirus 1. Science 255: 1718-1720.

Caswell, P.T., Chan, M., Lindsay, A.J., McCaffrey, M.W., Boettiger, D., and Norman, J.C. (2008) Rab-coupling protein coordinates recycling of alpha5beta1 integrin and EGFR1 to promote cell migration in 3D microenvironments. J Cell Biol 183: 143-155.

Caswell, P.T., Vadrevu, S., and Norman, J.C. (2009) Integrins: masters and slaves of endocytic transport. Nat Rev Mol Cell Biol 10: 843-853.

Cooray, S. (2004) The pivotal role of phosphatidylinositol 3-kinase-Akt signal transduction in virus survival. J Gen Virol 85: 1065-1076.

Esfandiarei, M., Luo, H., Yanagawa, B., Suarez, A., Dabiri, D., Zhang, J., *et al* (2004) Protein kinase B/Akt regulates coxsackievirus B3 replication through a mechanism which is not caspase dependent. J Virol 78: 4289-4298.

Hamasaki, M., Araki, N., and Hatae, T. (2004) Association of early endosomal autoantigen 1 with macropinocytosis in EGF-stimulated A431 cells. Anat Rec A Discov Mol Cell Evol Biol 277: 298-306.

Heikkila, O., Susi, P., Tevaluoto, T., Harma, H., Marjomaki, V., Hyypia, T., *et al* (2010) Internalization of coxsackievirus A9 is mediated by {beta}2-microglobulin, dynamin, and Arf6 but not by caveolin-1 or clathrin. J Virol 84: 3666-3681.

This article is protected by copyright. All rights reserved.

Hewlett, L.J., Prescott, A.R., and Watts, C. (1994) The coated pit and macropinocytic pathways serve distinct endosome populations. J Cell Biol 124: 689-703.

Huttunen, M., Waris, M., Kajander, R., Hyypia, T., and Marjomaki, V. (2014) Coxsackievirus A9 infects cells via nonacidic multivesicular bodies. J Virol 88: 5138-5151.

Ivaska, J., and Heino, J. (2011) Cooperation between integrins and growth factor receptors in signaling and endocytosis. Annu Rev Cell Dev Biol 27: 291-320.

Kankaanpää, P., Paavolainen, L., Tiitta, S., Karjalainen, M., Paivarinne, J., Nieminen, J., *et al* (2012) BioImageXD: an open, general-purpose and high-throughput image-processing platform. Nat Methods 9: 683-689.

Karjalainen, M., Kakkonen, E., Upla, P., Paloranta, H., Kankaanpaa, P., Liberali, P., *et al* (2008) A Raft-derived, Pak1-regulated entry participates in alpha2beta1 integrin-dependent sorting to caveosomes. Mol Biol Cell 19: 2857-2869.

Karjalainen, M., Rintanen, N., Lehkonen, M., Kallio, K., Maki, A., Hellstrom, K., *et al* (2011) Echovirus 1 infection depends on biogenesis of novel multivesicular bodies. Cell Microbiol 13: 1975-1995.

Liberali, P., Kakkonen, E., Turacchio, G., Valente, C., Spaar, A., Perinetti, G., *et al* (2008) The closure of Pak1-dependent macropinosomes requires the phosphorylation of CtBP1/BARS. EMBO J 27: 970-981.

Lill, N.L., and Sever, N.I. (2012) Where EGF receptors transmit their signals. Sci Signal 5: pe41.

Lund, K.A., Lazar, C.S., Chen, W.S., Walsh, B.J., Welsh, J.B., Herbst, J.J., *et al* (1990) Phosphorylation of the epidermal growth factor receptor at threonine 654 inhibits ligand-induced internalization and down-regulation. J Biol Chem 265: 20517-20523.

Marjomäki, V., Pietiäinen, V., Matilainen, H., Upla, P., Ivaska, J., Nissinen, L., *et al* (2002) Internalization of echovirus 1 in caveolae. J Virol 76: 1856-1865.

Mattila, E., Pellinen, T., Nevo, J., Vuoriluoto, K., Arjonen, A., and Ivaska, J. (2005) Negative regulation of EGFR signalling through integrin-alpha1beta1-mediated activation of protein tyrosine phosphatase TCPTP. Nat Cell Biol 7: 78-85.

Moro, L., Dolce, L., Cabodi, S., Bergatto, E., Boeri Erba, E., Smeriglio, M., *et al* (2002) Integrin-induced epidermal growth factor (EGF) receptor activation requires c-Src and p130Cas and leads to phosphorylation of specific EGF receptor tyrosines. J Biol Chem 277: 9405-9414.

Ogiso, H., Ishitani, R., Nureki, O., Fukai, S., Yamanaka, M., Kim, J.H., *et al* (2002) Crystal structure of the complex of human epidermal growth factor and receptor extracellular domains. Cell 110: 775-787.

This article is protected by copyright. All rights reserved.

Pietiäinen, V., Marjomäki, V., Upla, P., Pelkmans, L., Helenius, A., and Hyypia, T. (2004) Echovirus 1 endocytosis into caveosomes requires lipid rafts, dynamin II, and signaling events. Mol Biol Cell 15: 4911-4925.

Platta, H.W., and Stenmark, H. (2011) Endocytosis and signaling. Curr Opin Cell Biol 23: 393-403.

Rintanen, N., Karjalainen, M., Alanko, J., Paavolainen, L., Maki, A., Nissinen, L., *et al* (2012) Calpains promote alpha2beta1 integrin turnover in nonrecycling integrin pathway. Mol Biol Cell 23: 448-463.

Ruusuvuori, P., Paavolainen, L., Rutanen, K., Maki, A., Huttunen, H., and Marjomaki, V. (2014) Quantitative analysis of dynamic association in live biological fluorescent samples. PLoS One 9: e94245.

Siljamaki, E., Rintanen, N., Kirsi, M., Upla, P., Wang, W., Karjalainen, M., *et al* (2013) Cholesterol dependence of collagen and echovirus 1 trafficking along the novel alpha2beta1 integrin internalization pathway. PLoS One 8: e55465.

Sorkin, A., and Goh, L.K. (2008) Endocytosis and intracellular trafficking of ErbBs. Exp Cell Res 314: 3093-3106.

Turkki, P., Makkonen, K.E., Huttunen, M., Laakkonen, J.P., Yla-Herttuala, S., Airenne, K.J., *et al* (2013) Cell susceptibility to baculovirus transduction and echovirus infection is modified by protein kinase C phosphorylation and vimentin organization. J Virol 87: 9822-9835.

Upla, P., Marjomaki, V., Kankaanpaa, P., Ivaska, J., Hyypia, T., Van Der Goot, F.G., *et al* (2004) Clustering induces a lateral redistribution of alpha 2 beta 1 integrin from membrane rafts to caveolae and subsequent protein kinase C-dependent internalization. Mol Biol Cell 15: 625-636.

Ward, E.S., Zhou, J., Ghetie, V., and Ober, R.J. (2003) Evidence to support the cellular mechanism involved in serum IgG homeostasis in humans. Int Immunol 15: 187-195.

Wells, A., Welsh, J.B., Lazar, C.S., Wiley, H.S., Gill, G.N., and Rosenfeld, M.G. (1990) Ligand-induced transformation by a noninternalizing epidermal growth factor receptor. Science 247: 962-964.

Wiley, H.S. (2003) Trafficking of the ErbB receptors and its influence on signaling. Exp Cell Res 284: 78-88.

Wiley, H.S. (1988) Anomalous binding of epidermal growth factor to A431 cells is due to the effect of high receptor densities and a saturable endocytic system. J Cell Biol 107: 801-810.

Wiley, H.S., Herbst, J.J., Walsh, B.J., Lauffenburger, D.A., Rosenfeld, M.G., and Gill, G.N. (1991) The role of tyrosine kinase activity in endocytosis, compartmentation, and down-regulation of the epidermal growth factor receptor. J Biol Chem 266: 11083-11094.

This article is protected by copyright. All rights reserved.

Wong, W.R., Chen, Y.Y., Yang, S.M., Chen, Y.L., and Horng, J.T. (2005) Phosphorylation of PI3K/Akt and MAPK/ERK in an early entry step of enterovirus 71. Life Sci 78: 82-90.

Yu, X., Miyamoto, S., and Mekada, E. (2000) Integrin alpha 2 beta 1-dependent EGF receptor activation at cell-cell contact sites. J Cell Sci 113 (Pt 12): 2139-2147.

Zhang, H., Li, F., Pan, Z., Wu, Z., Wang, Y., and Cui, Y. (2014) Activation of PI3K/Akt pathway limits JNK-mediated apoptosis during EV71 infection. Virus Res 192: 74-84.

This article is protected by copyright. All rights reserved.

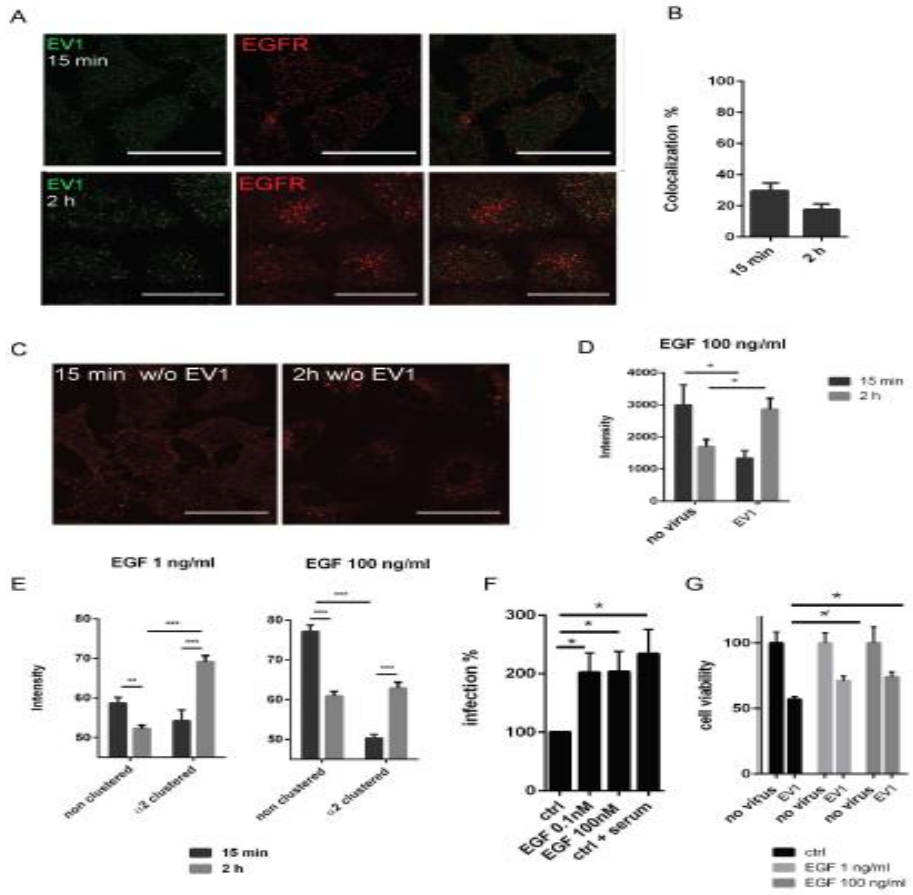

Figure 1. EV1 leads to accumulation of EGFR in cells during EGF stimulation. A) A549 cells immunolabeled for EV1 (green) and EGFR (red) after EV1 internalization during EGF treatment for 15 min and 2 h (100 ng/ml). B) Colocalization between EV1 (green) and EGFR (red) was quantified using BioImageXD from confocal sections from 160 to 180 cells. The ratio of colocalized voxels out of all green signal voxels above a set threshold was calculated. C) Confocal images of EGFR labeling of EGF-stimulated (100 ng/ml) cells without EV1 treatment. D) Quantification of EGFR signal during EGF stimulation with or without EV1 infection for 15 min and 2 h, calculated from 144 to 180 cells. E) Quantification of EGFR intensity with and without α2-integrin antibody clustering from SAOS- α2β1 cells with low and high dose of EGF. Twenty cells were used in the calculations from confocal sections for each case. F) Effect of EGF stimulation (0.1 nM and 100 nM) on EV1 infection percentage quantified 7 h p.i. from SAOS- α2β1 cells. Control infection after starvation (Ctrl) and under normal serum conditions (ctrl+serum) are shown. The results are mean values of three experiments. G) ATP levels monitored after 20 h of EV1 infection during stimulation of low (1 ng/ml) or high (100 ng/ml) EGF. The results are representative of 3 independent experiments. (* = P > 0.05) (**= P > 0.01) (***= P > 0.001) Scale bars 20 µm. The mean values and SEM are shown (standard error of means).

This article is protected by copyright. All rights reserved.

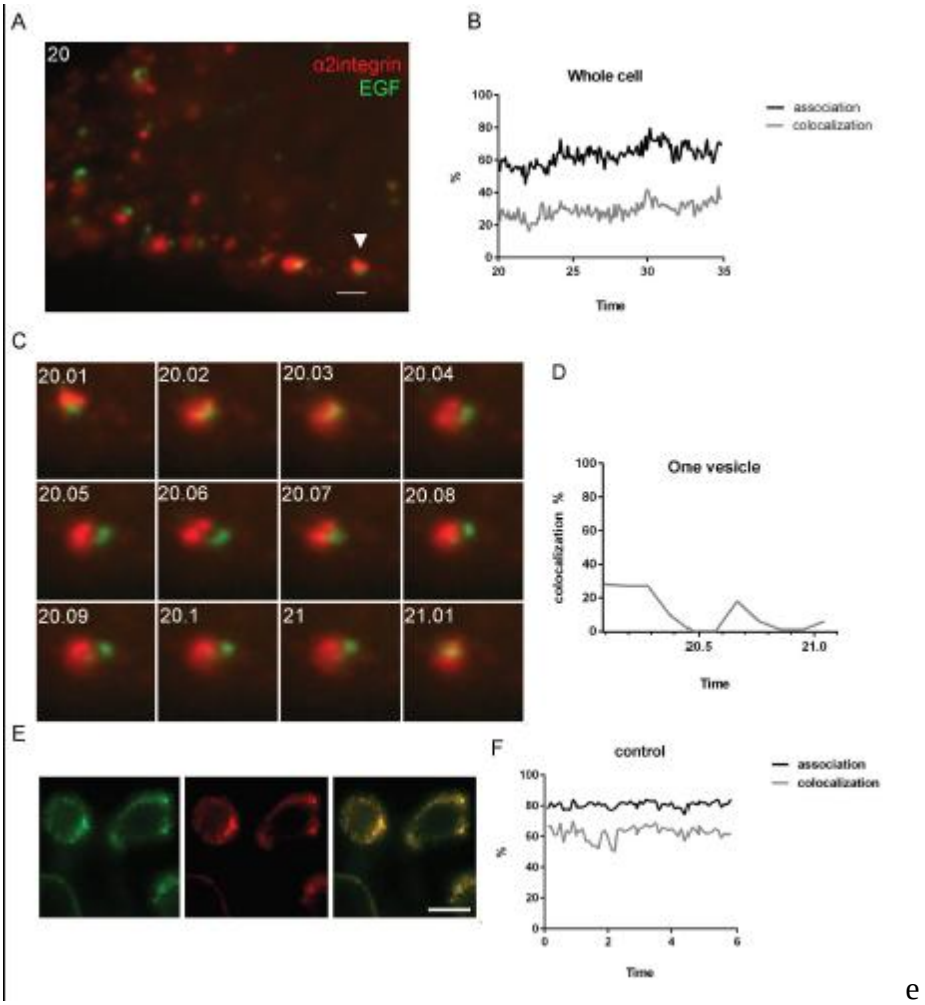

Figure 2. Virus receptor clustering and EGF stimulation leads to separate vesicles that are dynamically associated but not colocalizing with each other. A) A549 cells after α2β1 integrin (red) clustering and internalization imaged together with biotinylated EGF (green) between 20 min and 35 min p.i. in a wide-field microscope at 37C. Scale bar, 2μM. B) Quantification of association and colocalization of α2β1 integrin and EGF labels during 20 to 35 min p.i in the cell C) Snap shots and colocalization analysis (D) of live imaging of α2β1 integrin and EGF positive vesicles situated close by, between 20 to 21 min p.i. E and F) Colocalization control of α2β1 integrin after clustering and internalization and labelling with two different alexa dyes against the same integrin. Quantification of colocalization and association (F) between α2β1 integrin labelled with two different alexa dyes and imaged during 6 min. Scale bar, 10 μM Time lapse videos for A and C can be found from the supplemental data.

This article is protected by copyright. All rights reserved.

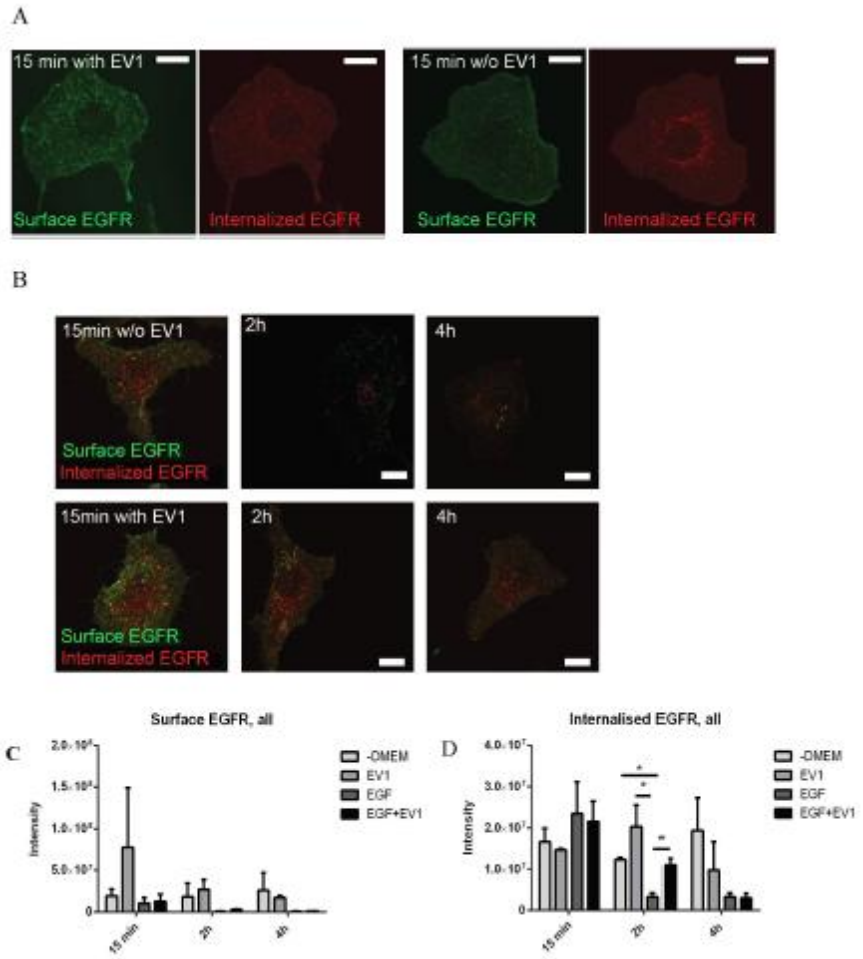

Figure 3. EV1 treatment slows down EGFR down-regulation. Serum starved A549 cells immunolabeled for surface (green) and intracellular (red) EGFR pools with and without EV1 internalization (A). B) Serum starved EGF stimulated A549 cells with and without simultaneous EV1 treatment. Quantification of the intensity of signal coming from the surface-associated EGFR (C) and internalized EGFR pools (D). Scale bars 10µm. Confocal images are representative of two independent experiments with 10 cells quantified from different experiments. The cells were treated with cycloheximide in all experiments in order to prevent any signal from newly synthesized EGFR. Scale bars 10µm.

This article is protected by copyright. All rights reserved.

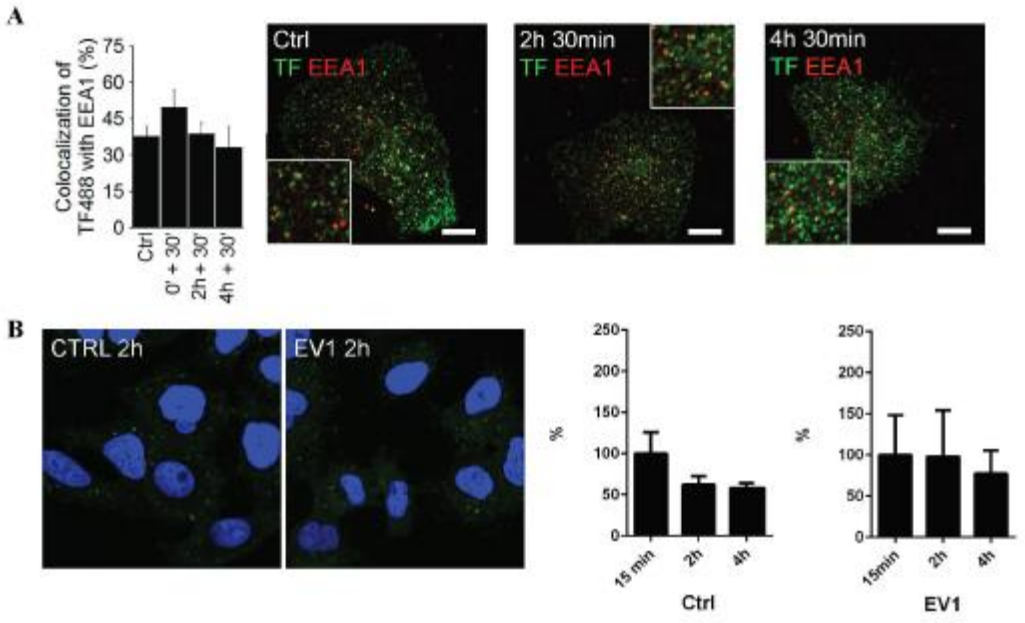

Figure 4. EV1 treatment has no effect on transferrin recycling or fluid phase uptake. A) Analysis of colocalization between the internalized Alexa488-labeled transferrin (green) (0.25 mg/ml) and the early endosomal marker EEA1. After a pulse of transferrin for 30 min and a chase for 2 or 4 h the colocalization was quantified from confocal images. Altogether, 10 cells from 2 independent experiments were quantified. Ctrl stands for a 30 min pulse without EV1 and "0´+ 30´" stands for the 30 min pulse with EV1. Blow-up images show in greater detail the distribution of internalized transferrin and EEA1. B) A high amount of mouse IgG (1 mg/ml) was added in cells for a 15 min pulse and then chased for 20 min at 2 and 4 h time points of EV1 treatment. Internalized IgG was detected by anti-mouse Alexa 488 conjugates and quantified. Examples of control cells and cells after EV1 treatment for 2 h are on the left. The experiment was done two times and 40 cells were quantified from confocal images. Scale bars 10µm.

This article is protected by copyright. All rights reserved.

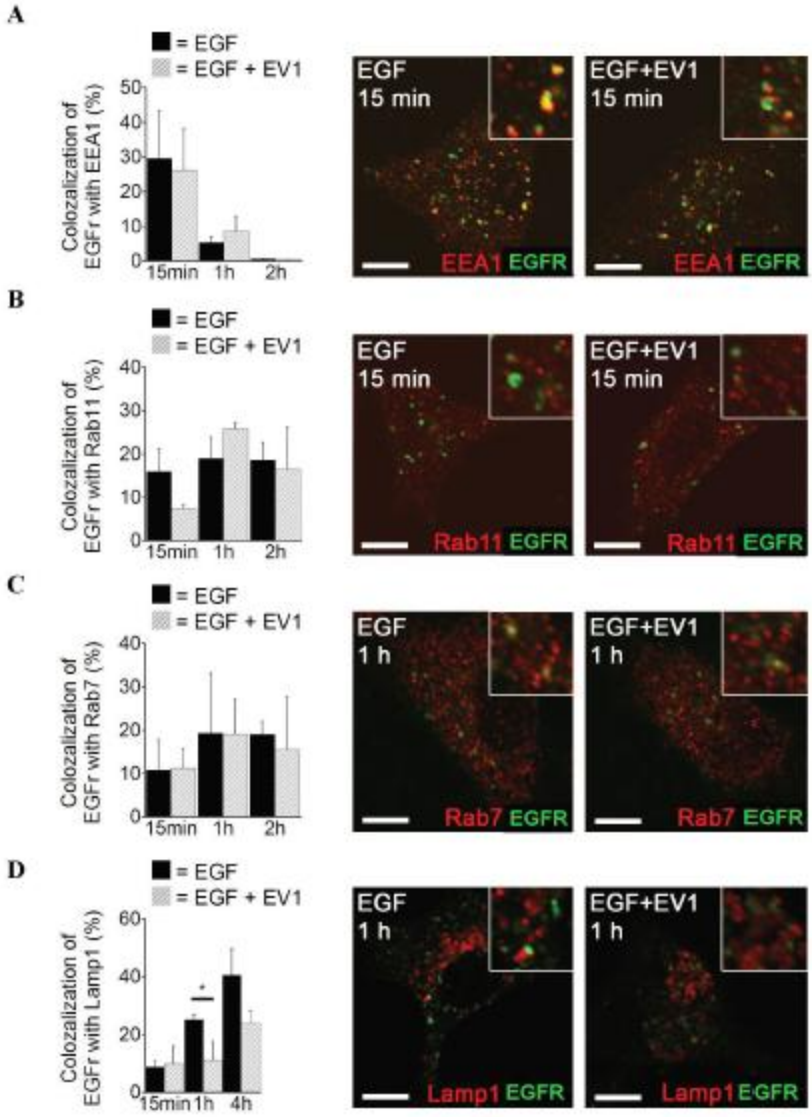

Figure 5. EV1 treatment causes a small reduction in EGFR colocalization with Rab11-positive recycling endosomes and lamp1-positive lysosomes. Colocalization analysis between EGFR and different endosomal markers such as A) the early endosomal marker EEA1, B) recycling endosome marker Rab11, C) late endosomal marker Rab7 and D) the lysosomal marker Lamp1 were performed. The quantification was performed from 3 experiments and from altogether 30 cells (mean values with SEM are shown). Representative examples from confocal images are shown on the right. Scale bars 10µm.

This article is protected by copyright. All rights reserved.

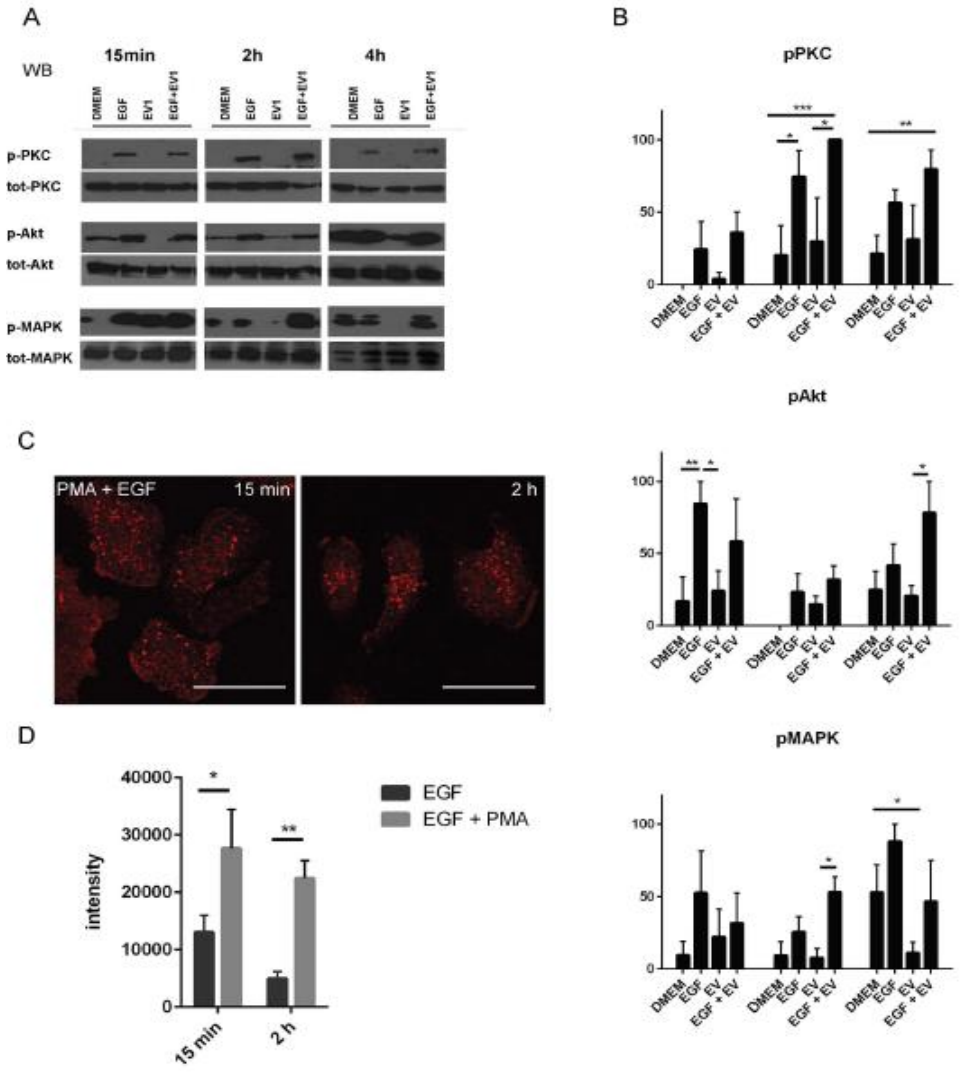

Figure 6. EV1 treatment moderately reduces EGFR downstream signaling. A) Immunoblotting of whole cells lysates against phosphorylated PKCα, Akt and 42/44 MAPK, and total proteins were performed. Similar number of cells on each sample were directly lysed in SDS-sample buffer, resolved in 10% SDS-PAGE and blotted. Results from one representative experiment are shown. B) Western blot signals were quantified with ImageJ software by normalizing the phosphorylated protein values to respective total protein values. The graphs show mean values ± SEM from three indedendent experiments. C) Confocal images of EGFR (red) signal during simultaneous PKC activation (with PMA) and EGF stimulation (100 ng/ml). D) Quantification of intensity of EGFR label in cells with EGF stimulation or PKC activation. Quantification was done from approximately 160 cells for each case.

This article is protected by copyright. All rights reserved.